Journal of Global Positioning Systems (2010)
Vol.9, No.1 :41-60
DOI: 10.5081/jgps.9.1.41

Journal of Global Positioning Systems
2010
© CPGPS

Adaptive Inter-Loop Aiding for Performance Improvements in Low CNIR Environments

Faisal A. Khan, Andrew Dempster, Chris Rizos
School of Surveying and Spatial Information Systems, University of New South Wales, Sydney, Australia

Abstract

Use of inter-loop aiding for improving tracking performance has been widely researched in recent years. However, most of the previously proposed aiding schemes rely on the assumption that the aiding loop remains unaffected by received interference. This paper argues that this may not always be the case. It is likely that the performance of the aiding loop may also degrade in the case where interference is received at the aiding carrier's frequency resulting in performance degradation of both aiding and aided loops. This paper proposes an aiding scheme that offers performance improvements in case interference corrupts both frequencies. Also, an algorithm is proposed that continuously updates the aided loop bandwidth to keep its jitter at a minimum. A relationship between the quality of the aiding signal and its effects on the performance of the aided loop is analysed. An adaptive Kalman filter-based implementation of the aiding architecture is proposed to improve the quality of aiding estimates. This implementation offers an improved margin against received interference. Simulation and real data results are presented that show improvements of 7 and 5 dB-Hz in this margin by employing the proposed aiding scheme with and without an adaptive Kalman filter.

Keywords: Loop aiding, Interference mitigation, Carrier phase jitter reduction, Tracking performance improvement

---

1. Introduction

Operation of Global Navigation Satellite Systems (GNSS) in classically difficult positioning environments has been an issue, particularly with regard to weak received signal levels and poor geometry conditions. Locata Corporation's Locata Positioning Network aims to address performance degradations in such situations. A Locata Network (LocataNet) is comprised of time-synchronised terrestrial transceivers (called LocataLites), operating in the 2.4GHz ISM band and transmitting signals appropriate for positioning. Use of time-synchronised transmitters allows single point positioning with centimetre level accuracy. Each LocataLite includes a dual-antenna transmitter; with each antenna (A1 and A2) transmitting positioning signals at two different frequencies (S1 and S6). This allows a Locata rover receiver to track four carriers (A1S1, A2S1, A1S6 and A2S6) from each of the LocataLites. Operation in the ISM band permits signal transmission at much higher power levels than those received from GPS, and avoids any licence requirement. This makes the system feasible for deployment in many situations and environments. However, operation in the licence-free ISM band is vulnerable to RF interference (RFI) from various other devices legally using the same spectral band. Interference from these devices artificially elevates the noise floor, degrading Locata signal's carrier-to-noise and interference-ratio (CNIR). Therefore reception of Locata signals requires that special attention be paid to interference rejection/mitigation for optimal operation. There have been improvements in Locata's interference rejection capabilities in the released version (V3R4). However, it was identified in the authors' previous work (Khan et al., 2010) that received RFI can cause Locata to operate sub-optimally. In (Khan et al., 2010), it was identified that some inherent characteristics of the Locata network can be exploited to gain further improvements in terms of noise and interference mitigation. In this paper the authors propose and analyse an inter-loop aiding scheme which enables Locata to track signals with CNIR reduced by noise, unintentional interference and/or jamming.

In a carrier phase positioning system, the performance of a carrier loop dictates the quality of the phase measurements and consequently the quality of the final positioning solution. However, the carrier loop has been identified as the weakest link in a navigation receiver due to its vulnerability to received noise and interference. This received noise and interference degrades the performance of the carrier loop thereby affecting the quality of the measurements and the final solution. Locata, working on similar principles to GPS, can suffer from the similar issues in the presence of noise and interference that degrade the CNIR levels.

This paper presents an inter-loop aiding scheme that offers tracking loop performance improvement in such a situation. The concept of loop aiding using either external aids, e.g. from Inertial Navigation Systems (INS)) or internal aids (from another tracking loop), is not new. However, due to the potential advantages it offers, particularly the achieved margin against RFI, it still remains a very attractive topic of research. A number of techniques have been proposed (e.g. (Alban et al. 2003), (Megahed et al., 2009) and (Qaisar, 2009)) where Doppler aiding enhances loop performance under attenuated signal conditions or in the presence of received RFI. It is interesting to note that such methods have their own limitations. In the case of external aiding, limitations are imposed by imperfections of external aiding estimates, inter-system synchronisation, increased system costs etc. On the other hand, internal aiding relies on aiding estimates generated within the receiver from another loop tracking a carrier at a different frequency. These aiding schemes rely on the assumption that the aiding carrier is a better source for acquiring cleaner aiding estimates that can be used to enhance the aided carrier's tracking performance. This paper argues that this may not always be the case and identifies examples where the aiding based on such an assumption may actually degrade the performance of the aided loop. These situations may arise due to the corruption of the aiding carrier frequency by received noise and RFI or by multipath. In such situations, the aiding carrier loop may produce low quality aiding estimates that in turn corrupt the performance of the aided loop even if the aided carrier's frequency was not affected. In addition, this will remove any advantages that could have been available due to the availability of frequency diversity like improved ambiguity resolution, multipath diversity and etc.

Exploiting the availability of two carriers at each of the two frequencies S1 and S6, this paper offers a solution to this problem for Locata. The loop aiding scheme proposed here offers improvements in situations where either or both of the carrier frequencies are corrupted. The proposed scheme operates by continuously monitoring the tracking of each of the four carriers and selects the best performing loop as the aiding loop, based on a preset criterion. Selection is done in real-time in order to decrease the vulnerability of the aiding process to changing received noise and RFI as well as multipath situations. The proposed scheme offers relatively cleaner measurements from both frequencies even if one or both of the two frequencies are affected by received noise and interference. It is to be noted that in the case where carriers at both the frequencies are affected by the received noise and interference, the aiding estimates will be obtained from a noisy signal. Considering this situation, this paper investigates the effect of the aiding carrier's signal quality on the aided loop's performance. Also by recognising the fact that the aiding loop can contribute to the noise in the aided loop, use of Adaptive Kalman Filtering is suggested as a possible solution. It is discussed and shown through simulations and experimental results that the use of an Adaptive Kalman Filter helps to improve the performance of the proposed scheme. Also, it is identified that although inter-loop aiding allows the aided loop's bandwidth to be reduced for rejection of received noise and interference, it is not always best to operate the aided loop at the minimum possible bandwidth. It is shown that operation at this minimum bandwidth may actually increase the jitter produced by the aided loop. An algorithm is proposed that continuously updates the aided loop bandwidth to keep its jitter at a minimum.

The novel contributions of this paper can be summarised as:

1. Proposal and detailed analysis of an aiding scheme that offers tracking performance improvements if either or both of the carrier frequencies are affected by received noise and RFI.
2. Algorithm proposal for adaptive selection of aided loop bandwidth.
3. Investigation of the effect of the aiding carrier's signal quality on the aided loop's performance.
4. Kalman filter based inter-loop aiding implementation that offers:
   a. increased margin against received noise and interference
   b. improvement in terms of Minimum Achievable Jitter (MAJ), and
   c. resistance to an aided loop's performance degradation as the aiding signal quality degrades.

It is important to note that most previously published research papers present results of performance improvements using loop aiding schemes in terms of a phase lock loop's (PLL) estimated Doppler. This paper recognises the PLL's total phase jitter as its performance metric and presents the performance improvements in terms of this metric. In addition, this paper presents real data results that validate the proposed scheme.

After introducing the theme of the paper in section 1, section 2 presents a brief overview of the carrier phase jitter, a metric used to reflect the tracking loop's performance. Section 3 discusses the problem statement followed by the inter-loop aiding scheme proposal in section 4. Simulation results for the proposed scheme are then presented and discussed in Section 5. Section 6 discuses the adaptive Kalman filter based implementation of the proposed scheme and presents the corresponding simulation results. The proposed schemes are validated in section 7 using the real data. Finally section 8 concludes the paper.

2. Carrier Phase Jitter

The main mode of positioning for Locata is carrier phase positioning that relies on carrier phase measurements (CPM) originating from the carrier tracking loop (PLL). The quality of these measurements and eventually that of the final positioning solution is consequently influenced by the performance of the PLL. This performance can be evaluated in terms of the PLL's phase variance σ_{φ}^2, where σ_{φ} is the total phase jitter. This total phase jitter has been identified as a metric of tracking loop's performance (Gebre-Egziabher et al., 2005), (Razavi et al., 2008). A higher value of this jitter indicates noisier measurements and decreased stability of the tracking loop itself. This suggests that in order to improve the quality of the individual CPM and that of the final positioning solution as well as the loop stability, it is critical to reduce this total phase jitter.

This total phase jitter is composed of four significant components: the noise- and interference-induced jitter phase jitter σ_{φ_t}, the vibration-induced jitter σ_{φ_v}, the oscillator noise-induced jitter $\sigma_{\varphi_{osc}}$ and the dynamic stress error θ_d, which can be combined as follows (Irsigler and Eissfeller, 2002):

$$\sigma_{\varphi} = \sqrt{\sigma_{\varphi_t}^2 + \sigma_{\varphi_v}^2 + \sigma_{\varphi_{osc-Tx}}^2 + \sigma_{\varphi_{osc-Rx}}^2} + \frac{\theta_d}{3} \qquad (1)$$

The noise- and interference-induced jitter σ_{φ_t} reflects the effects of received noise and RFI on PLL operation, and can be given as (Irsigler and Eissfeller, 2002):

$$\sigma_{\varphi_t} = \sqrt{\frac{B_L}{C/(N_o + I)}\left(1 + \frac{1}{2T\,C/(N_o + I)}\right)} \qquad (2)$$

where C, N and I denote the carrier, noise and interference powers, $C/(N_o + I)$ denotes the CNIR, B_L denotes the loop bandwidth and T denotes the integration duration.

The vibration-induced phase jitter $\sigma_{\delta\varphi_v}$ is the oscillator's external phase noise caused when the platform, on which the receiver is mounted, is subjected to mechanical vibration. $\sigma_{\delta\varphi_v}$, for a third order PLL, can be given as (Irsigler and Eissfeller, 2002):

$$\sigma_{\delta\varphi_v} = \sqrt{2\pi f_o^2 \int_0^{\infty} \frac{k_g^2(\omega) G_g(\omega) \omega^4}{2.98 B_L^6 + \omega^6} d\omega} \qquad (3)$$

where f_o is the carrier frequency, k_g is the oscillator's g-sensitivity in parts-per-g, G_g is the single-sided vibration spectral density and ω is the vibration radian frequency. A third order loop is considered here as the same is used in current Locata rover receivers.

In contrast to $\sigma_{\delta\varphi_v}$, which reflects external phase noise, $\sigma_{\varphi_{osc-tx}}$ and $\sigma_{\varphi_{osc-rx}}$ reflect the oscillators' natural phase noises at the transmitter and the receiver ends respectively. Such phase noises, resulting from oscillator instabilities, can be given as (Irsigler and Eissfeller, 2002):

$$\sigma_{\varphi_{osc}} = \sqrt{2\pi f_o^2 \int_0^{\infty} \left[\frac{2\pi^2 h_{-2}}{\omega^4} + \frac{\pi h_{-1}}{\omega^3} + \frac{h_0}{2\omega^2}\right] \frac{\omega^6}{2.98 B_L^6 + \omega^6} d\omega} \qquad (4)$$

where, h_{-2}, h_{-1} and h_0 are the oscillator coefficients, which need to be derived experimentally.

Finally the dynamics stress error indicates the bias in the phase error induced due the platform movement. For a 3rd order loop, dynamics stress error can be given by (Irsigler and Eissfeller, 2002):

$$\theta_d = \frac{d^3R/dt^3}{1.728 B_L^3} \qquad (5)$$

where d^3R/dt^3 denotes the maximum 3rd order line-of-sight dynamics experienced by the receiver.

Trends of these individual sources of error against different values of loop bandwidth (B_L) are depicted in Fig. 1. A TCXO is used by both the Locata transmitter and receiver. Data for a generic TCXO and platform vibration, extracted from (Gebre-Egziabher et al., 2005) and (Singh et al., 1996) respectively have been used to plot the jitter profiles in Fig. 1. Plots assume a CNIR value of 35dB-Hz. Also 0.38g/s is assumed for dynamic stress errors as indicated by (Chiou et al., 2007) as the operational standard value for an automobile LOS dynamics. Carrier frequency and wavelength are assumed to be those of the Locata S1 carrier. Fig. 2 and 3 depict the total phase jitter plotted against B_L and CNIR. The heavy lines at 15° in these two figures denote the theoretical upper limit of total phase jitter, which has been defined for an acceptable operation of a PLL (Gebre-Egziabher et al., 2005), (Ward et al., 2006). Phase jitter values above 15° can be considered critical as they may indicate loss of lock.

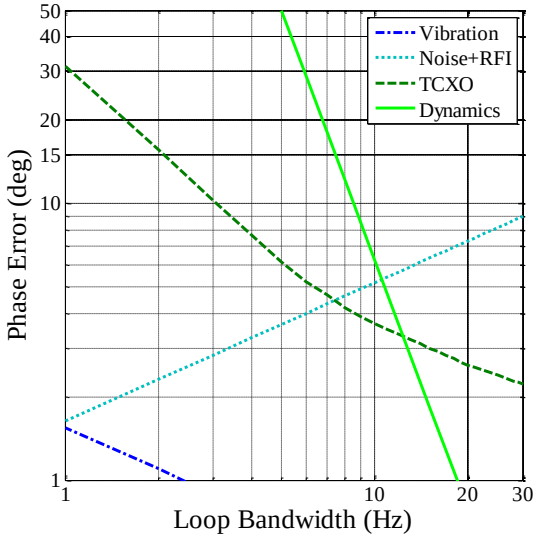

Figure 1: individual sources of error contributing to total phase jitter.

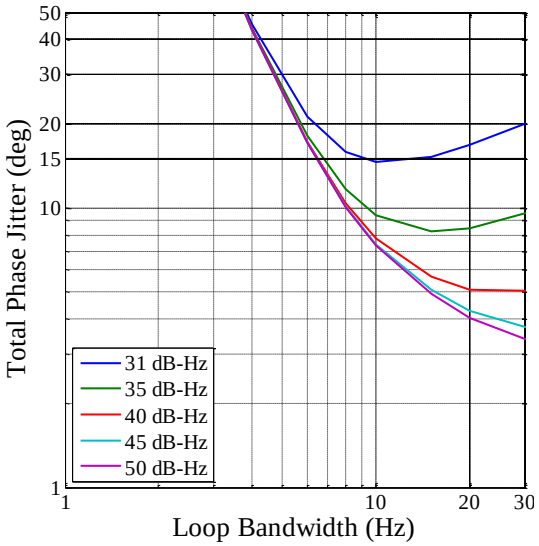

Figure 2: Theoretical total phase jitter against loop bandwidth for different received signal's CNIR (without loop aiding).

3. Problem Statement

The main goal here is to reduce the total phase jitter in order to:

1. be able to track signals and avoid loss of lock under degraded CNIR conditions. This will involve gaining some margin against received noise and interference. By reducing the total phase jitter, the loop is kept from operating near the 15° threshold. Therefore, an attempt to reduce the total phase jitter allows the loop to operate below the threshold and decreases the chances of losing lock.
2. obtain cleaner carrier phase measurements in the presence of received noise and interference by mitigating this noise entering the tracking loops. This consequently helps improve the quality of the final solution.
3. avoid cycle slips experienced due to received noise and interference. As Locata produces a solution using carrier phase positioning, the resolved ambiguity is of critical importance. Any cycle slip that may occur invalidates the resolved ambiguity making the carrier phase measurements biased and inaccurate. Some examples of Locata receivers experiencing cycle slips due to received noise and interference are reported in (Khan et al., 2010). Such occurrences of cycle slips can be explained by considering the discriminator output. This paper considers the use of $\tan^{-1}$ discriminator and its output is plotted in Fig. 4. It can be seen that $\tan^{-1}$

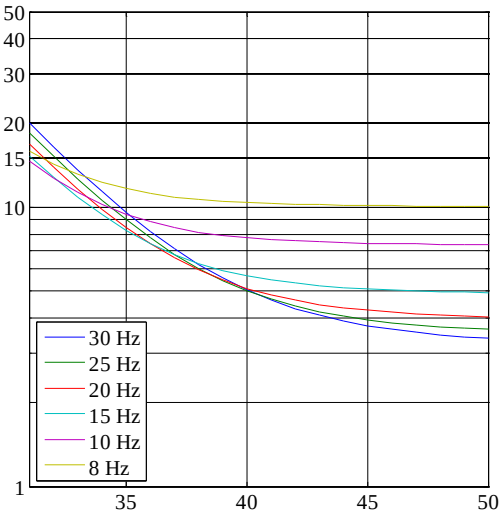

Figure 3: Theoretical total phase jitter against CNIR for different loop bandwidths (without loop aiding).

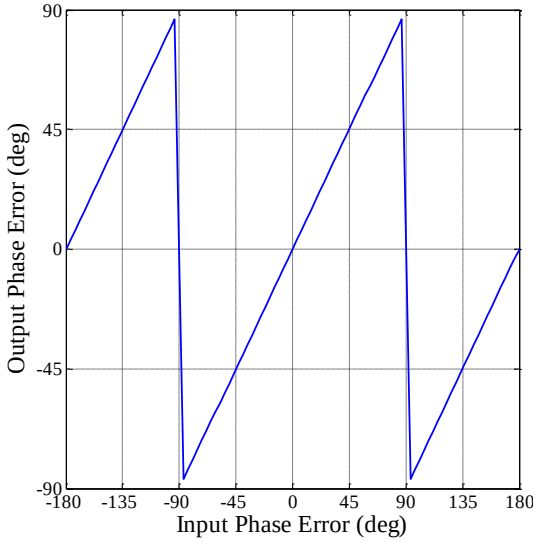

Figure 4: $\tan^{-1}$ phase discriminator output.

discriminator has a linear output for the input error less than ±90°. For an input phase error more than 90°, the discriminator may estimate an opposite phase error (a phase error with the same magnitude but opposite sign) to the actual input phase error, resulting in a cycle-slip. Such a situation is likely to occur when a signal with a low CNIR is tracked. This is due to the fact that tracking at low CNIR produces higher phase jitter contributed by larger input phase errors that can cause cycle slips. Also, at lower CNIR, the width of this linearity region decreases from ±90° due to the noise entering the tracking loops (Julien et al., 2005). This again contributes towards increasing the probability of cycle slip occurrence.

It is also interesting to note that phase jitter reduction is more critical for Locata than for GNSS. As can be noticed from Equations (3), (4) and (5) above, oscillator- and vibration-induced phase jitter and dynamic stress error are proportional to carrier frequency. Most of the GNSS carriers lie in L band (1 – 1.5 GHz), while Locata employs carriers in the ISM band (2.4 – 2.5 GHz). This suggests that for the same quality of oscillator or for the same extent of platform vibration and dynamics, Locata will experience much more jitter than any GNSS receiver (e.g. approximately 1.5 times more jitter than in case of GPS L1 signal). This makes it further essential to mitigate this jitter to improve the receiver performance and integrity.

Equation (2) suggests that, for a given CNIR, phase jitter reduction can be achieved by minimising B_L. This is due to the fact that in such a scenario, B_L becomes narrow enough to reject more noise. However, for smaller B_L values, phase errors due to oscillator induced jitter (including that due to vibration) and dynamics stress tend to increase as indicated by Equations (3), (4) and (5), and depicted in Fig. 1. These errors set a lower limit to which the B_L can be reduced. This defines the classic trade-off that exists between noise rejection and reduction of oscillator and dynamics induced errors.

A possible solution to this involves the reduction of the errors that set a lower limit on B_L. This allows further reduction in B_L facilitating further noise rejection. For conventional loops this lower limit varies between 10 – 18Hz depending on the application. However, if the PLL can be aided by providing estimates of these errors, it does not need to track these errors and should be able to operate with a smaller B_L. Inertial loop aiding has long been employed to achieve this purpose, where Doppler estimates are externally estimated and are provided to PLL. In this case the lower limit is set by the oscillator- and vibration-induced errors and the imperfections of dynamics estimates provided by the inertial navigation system (INS) (Gebre-Egziabher et al., 2005). However, if the aid is obtained from another carrier tracking loop on board the receiver, it helps to estimate errors due to receiver clock and vibrations, in addition to dynamics-induced errors (Fontana et al., 2001). This is possible if the carriers at more than one frequency are tracked by the receiver and the same can be illustrated by considering Equations (3), (4) and (5). These equations suggest that the dynamic stress errors and the oscillator- and vibration-induced jitter are all directly related to the carrier frequency. If these errors can be obtained from one PLL, the same can be used to aid another PLL by scaling them using the ratio of the carrier frequencies of the signal tracked by the two PLLs, operating in the same receiver and tracking signals from the same transmitter. In such schemes, one of the available carrier loops that has been identified as less vulnerable to tracking errors (e.g. due to high transmit power levels or availability of a data-less carrier allowing longer integration times etc) is used to provide aid to the more vulnerable loop. Such schemes offer the advantages of inter-loop aiding without requiring any external assistance. These rely on an underlying assumption that the aiding carrier will be tracked in a situation better than the aided carrier and therefore the latter can rely on the former for obtaining clean estimates better than those it can generate by itself. Typical examples could be L5 aiding L1 (Megahed et al., 2009) or L2 aiding L1 (Qaisar, 2009). However, it is straightforward to note that this may not always be the case. If the noise and interference received at the aiding carrier's frequency is higher than at the aided carrier's frequency, aiding may provide worse estimates than the aided loop can generate itself. This leaves inter-loop aiding still vulnerable to received interference. In addition, in such situations where the aiding frequency receives more noise and interference, the benefits of the availability of dual frequency measurements are lost.

4. Scheme Proposal

This paper proposes a loop aiding architecture resolving the above-mentioned issues for Locata. This is achieved by exploiting the availability of four carriers (A1S1, A1S6, A2S1 and A2S6) at two different frequencies (namely S1 and S6) from each of the two antennas (namely A1 and A2). First the loop aiding is explained mathematically and then starting with a basic loop-aiding architecture, a final architecture is proposed going through different modifications considering the possible issues. Progress through different modifications helps justify the final proposed architecture.

4.1 Loop aiding

Before proposing a loop-aiding architecture, it's useful to explore how loop aiding works mathematically. The signal reaching the tracking loops can be represented by:

$$y(t) = A\sin(2\pi(f_{rel} + f_{osc} + f_{vib} + f_{oth})t + \theta) \quad (6)$$

where

A = received signal amplitude

f_{rel} = Doppler frequency due to platform dynamics

f_{osc} = oscillator-induced frequency errors

f_{vib} = vibration-induced frequency errors

f_{oth} = frequency errors due to troposphere, noise and interference and other unmodelled errors

θ_i = carrier phase at phase detector

The aiding loop generates an estimate of the incoming signal using a wider B_L. As the signals reaching the aiding and the aided loops mainly differ due to their carrier frequencies, a scaled version of these estimates generated by the aiding loop can be provided to the aided loop. The scaling factor here is the ratio of the aiding and aided loop carrier frequencies. It is to be noted that the aiding and aided loops may track signals with the same carrier frequency. In this case, this ratio becomes unity. The aided loop generates the incoming signal's replica using its own estimates and those obtained from the aiding loop and these can be given as:

$$\hat{y}(t) = \sin(2\pi(\hat{f}_{rel} + \hat{f}_{osc} + \hat{f}_{vib} + \hat{f}_{oth})t + \phi) \quad (7)$$

where $\hat{f}_{rel}$, $\hat{f}_{osc}$, $\hat{f}_{vib}$ and $\hat{f}_{oth}$ denote the estimated error quantities. Now the discriminator at the aided loop uses the received signal and the locally generated replica to generate the error signal given by:

$$y\hat{y}(t) = \sin(2\pi(f_{est} + f''_{oth})t + \psi) \quad (8)$$

Two quantities f_{est} and f''_{oth} are introduced here which denote the estimation errors and noise, interference and other unmodelled error differences. Effectively the aided loop now has to track these residual errors $f_{est} + f''_{oth}$ which are (relatively) less than the actual errors. As a result a very small B_L can be used by the aided loop to track these errors, using which it can reject more noise and interference.

It must be emphasised that in this architecture, aiding is obtained from another loop, instead of some external device such as an INS. For this reason, although the errors due to platform dynamics, vibration and local oscillator (receiver clock) are reduced, additional phase errors due to noise and interference are induced from the aiding loop. This introduces a composite noise error in the replica signal generated by the aided loop's NCO. This composite error can be expressed as:

$$\sigma^2_{\varphi_o,comp} = \sigma^2_{\varphi_o(aiding)} + \sigma^2_{\varphi_o(aided)} \quad (9)$$

The total phase jitter of the aided loop will consist of these composite errors in addition to estimation and other unmodelled errors. Therefore Equation (9) suggests a lower bound on the total phase jitter of the aided loops, as these will be present even if the signal dynamics estimates are very close to the actual values.

Also, Equation (9) suggests a relationship between the aided loop's total phase jitter and the quality of the signal tracked by the aiding loop. For the aided loop to perform better would require a relatively interference-free and less noisy estimate from the aiding loop. Where the aiding estimates are corrupted by received interference, the aided loop's performance will be degraded. A loss of lock can also occur for the aided loop in this situation depending upon the quality of the aiding information. Such a situation can be predicted using Equations (2) and (9) if the individual CNIR values are known.

The above discussion can be summarised as follows:

4. An aiding loop operates with a wider (B_L) and estimates dynamics-induced errors and vibration- and oscillator-induced jitters.
5. An aided loop operates with a narrower B_L to reject noise and interference producing cleaner measurements. Operation at a narrow B_L is made possible by using the error estimates from the aiding loop.
6. If the aiding loop receives noise and interference, the same would be reflected in its error estimates. Measurements from the aided loop would also be corrupted when using these noisy estimates from the aiding loop.

4.2 Architectures

Starting from a conventional aiding architecture, Fig. 5 depicts a basic loop-aiding architecture that resembles in functionality the architectures defined in (Megahed et al., 2009) and (Qaisar, 2009). Here the A1S1 loop aids the A1S6 loop, and the A2S6 loop aids the A2S1 loop. In a situation where interference is received on the S1 frequency only, cleaner measurements on this frequency can be obtained from an A2S1 loop that, by using the aiding estimates from A2S6 loop, is able to operate at a smaller bandwidth rejecting more noise and interference. Similarly, the A1S6 loop can be used to obtain cleaner measurements in the case where received noise corrupts carriers at the S6 frequency only. This architecture allows obtaining of cleaner measurements at both the frequencies by using the narrow B_L aided loops. However, as discussed above, if the received noise and interference corrupt both carriers, this architecture

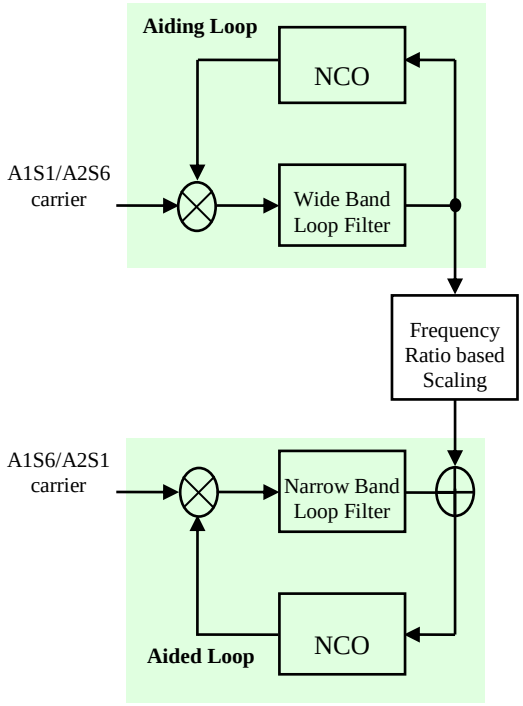

Figure 5: Generic aiding loop architecture.

produces noisy measurements at both frequencies negating the advantages offered by loop aiding.

Fig. 6 depicts a modification of the previous architecture. Here the four carriers are divided in to two groups: aiding and aided. One carrier at each frequency is allocated to the aiding group (say A1S1 and A2S6), and the remaining two carriers (A1S6 and A2S1) are allocated to the aided group. Both the loops tracking "aided" group carriers receive error estimates from one of the carriers in the "aiding" group. This aiding carrier is selected as the one least affected by the received noise and interference. For instance, if the received noise and interference corrupts measurements at S1, both aided loops (tracking A1S6 and A2S1) switch to the A2S6 loop to obtain aiding estimates and generate cleaner measurements. Similarly A1S1 will be used to obtain aiding, in the case received noise and interference affects S6. In the case where both frequencies are affected, both the aided loops switch to the aiding loop at the least affected frequency making their estimates relatively less noisy. Using this scheme, the least affected of the two aiding loops will be adaptively selected to aid both aided loops, where the aiding loop will handle dynamics and errors due to other sources using a wider B_L and the aided loop will reject noise and interference using narrow B_L.

This architecture assumes that one of the two available carriers at each frequency needs to be selected as the aiding carrier. This selection is done by considering the effects of received noise and interference as well as

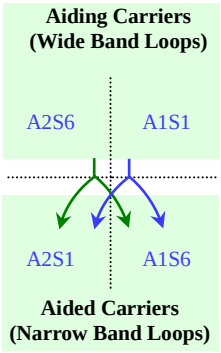

Figure 6: Inter-loop aiding architecture. Aiding obtained from A1S6 if $CNIR_{A1S6}$>$CNIR_{A2S6}$ and vice versa.

multipath. In a real-world scenario, multipath needs to be considered in addition to received noise and interference as a factor affecting tracking loop's performance. A destructive multipath degrades the received signal's CNIR increasing the thermal jitter. The above discussed architecture suggests that if the noise and interference is received at the S1 frequency, both aided loops will switch to A2S6. However, if the carriers from the A2 antenna are affected by multipath, any aiding received from the A2S6 loop will corrupt the measurements from the aided loops as well. It is highly likely that the performance of the loops tracking carriers from the two different antennas will be differently affected by the multipath, with one performing better than the other (this is the reason two antennas are used). This suggests that the carriers be allocated to the aiding and the aided groups adaptively, in real-time, by selecting a better performing loop in terms of multipath and received noise and interference rejection. This calls for an eligibility criterion for selecting aiding loops. Total phase jitter is a metric of loop performance. This jitter is composed of oscillator- and vibration-induced jitter and dynamics stress errors. Each of these contributors induces a similar value of jitter for all four carriers tracked from the same LocataLite. This is because the jitter due to these contributors varies depending on the carrier frequencies S1 and S6 and the ratio S1/S6 is very close to unity. All the other parameters affecting these jitter sources remain the same for all four carriers. The only factor that can make the total phase jitters, for the four carriers, substantially different from each other is the noise- and interference-induced jitter. This is due to the fact that carriers at different frequencies are affected differently by the received noise and interference. A received signal's CNIR is the parameter that reflects the effects of received noise and interference. Also, CNIR reflects the constructive or destructive nature of multipath; a constructive multipath improves the signal's CNIR reducing noise and interference induced jitter. This discussion implies that the CNIR is an eligible candidate for selecting the aiding loop(s).

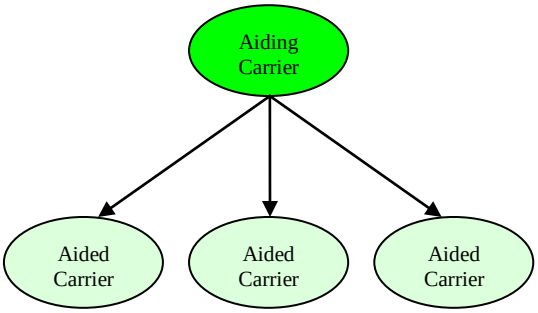

Figure 7: Modified inter-loop aiding architecture. Carrier with the best CNIR is selected for providing aiding estimates to the rest of the three carriers.

The above-mentioned architecture offers at least one cleaner measurement on each of the two frequencies, using narrow B_L aiding loops, even if both the frequencies are corrupted by received noise and RFI. This architecture can further be modified in order to obtain a total of three cleaner measurements on two different frequencies. This is done by selecting only one of the loops as the aiding loop providing error estimates to all the other loops that produce cleaner measurements using a narrow B_L. The architecture, as depicted in Fig. 7, proposes that the CNIR from all four carriers be continuously monitored and the loop with the highest CNIR be selected as the aiding loop. Again, CNIR is maintained as the criteria for selecting the aiding loop due to the reasons mentioned above. It should be noted here that the change in B_L only affects the jitter experienced and not the CNIR i.e. the same CNIR value is reported by the loop irrespective of the employed B_L. The Variance Summing Method (VSM) was used for determining CNIR in simulations reported in this paper. Where both the frequencies are corrupted by received noise and RFI, CNIR for all four carriers will degrade. In such a scenario, by selecting the carrier with the best CNIR, the aiding loop producing the least noisy estimates is selected as the aiding loop. This modification adds simplicity to the proposed architecture. Also, the number of cleaner measurements increase from two to three due to the fact that three carrier tracking loops (as compared to two in case of previous architecture) operate employing a narrower B_L, offering noise rejection and resulting in cleaner measurement from each of these three loops.

5. Scheme Implementation

In order to analyse the proposed architecture, Locata signals were simulated according to the available specifications (Barnes et al., 2005), and were processed using a software receiver. Simulations considered the same coordinates for LocataLite positions at which the LocataLites are positioned in a real network setup at University of New South Wales (UNSW). Monte Carlo simulations were performed to evaluate the performance of the proposed scheme where different scenarios were simulated considering interference on either or both of the frequencies. WiFi devices operating in the 2.4GHZ ISM band have been identified as the most likely potential interferer for Locata (Khan et al., 2010). WiFi signals are 20MHz wide and therefore generate wide-band interference for Locata. Also, due to the artificially raised noise floor in this band, Locata experiences increased wide-band-noise levels. Considering these reasons, wide-band interference was considered for the simulations. For maximum LOS dynamic stress, simulations assumed a value of j_{max}=0.38g/s. Multipath effects were included by considering a single-dominant reflector with varying parameters (reflection coefficient and time delay). This was done considering the relative geometry of the receiver and multiple virtual reflectors (all represented by one single reflector with time varying characteristics).

5.1 Unaided loop performance

In order to determine the receiver performance in the absence of loop aiding, a conventional (unaided) loop was used to track the simulated signals with different CNIR. Results of this scenario served as a reference for comparing the results of the proposed architecture. Fig. 8 and 9 depict the resulting phase jitter which is plotted against B_L and CNIR. As suggested by the theory, it can be readily noticed here that the phase jitter is significantly dependent on B_L for all values of CNIR. Fig. 8 shows that for smaller B_L the phase jitter curves for different values of CNIR tend to converge. This convergence occurs due to the fact that for narrower B_L, noise- and interference-induced errors become less dominant as compared to errors induced by the other sources which are common for all the curves. This convergence point is jointly determined by the signal dynamics (due to platform dynamics, clock and vibration induced noise) and CNIR. It is important to note that all the converged curves cross the 15° threshold at similar values of B_L. This suggests that at the narrow B_L for these curves, the phase jitter threshold is crossed independently of the received signal's CNIR. Although at this low B_L the noise rejection is at its maximum, the signal dynamics induced errors become dominant enough to keep the jitter in the vicinity of the 15° threshold for all values of received CNIR. This makes the loop highly vulnerable to loss of lock due to even a slight increase in signal dynamics induced errors. It was found that with B_L narrowed further below 9Hz to reject more noise and interference, a carrier loop was not able to maintain lock. In order to decrease a loop's vulnerability, loop aiding is employed and results are presented in the following sub-sections.

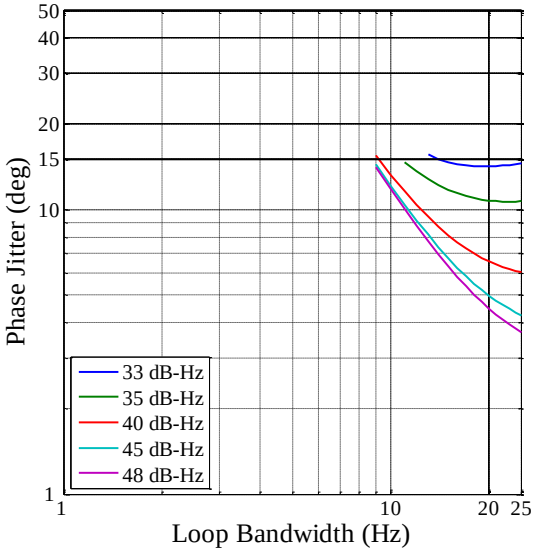

Figure 8: Phase Jitter against Loop Bandwidth for Different CNIR (Without Loop Aiding). Results obtained using simulated data.

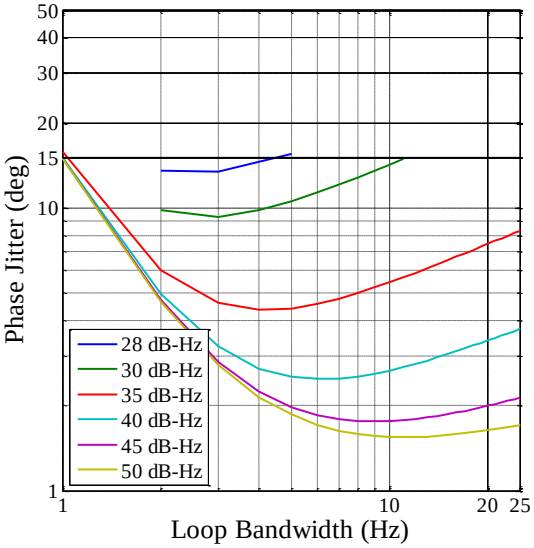

Figure 10: Phase Jitter against Loop Bandwidth for Different CNIR (With Loop Aiding). Results obtained using simulated data.

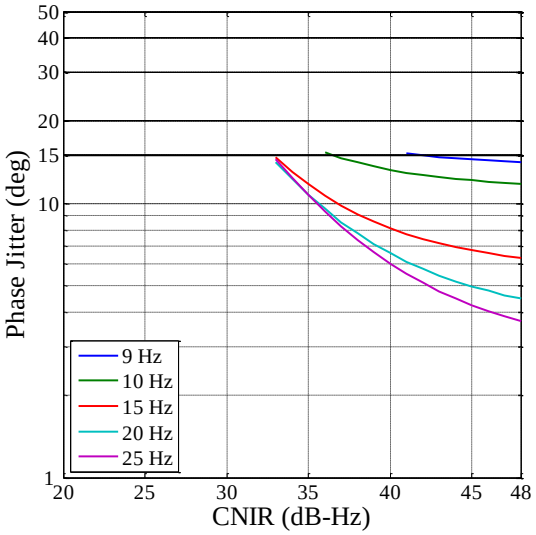

Figure 9: Phase jitter against CNIR for different loop bandwidths (without loop aiding). Results obtained using simulated data.

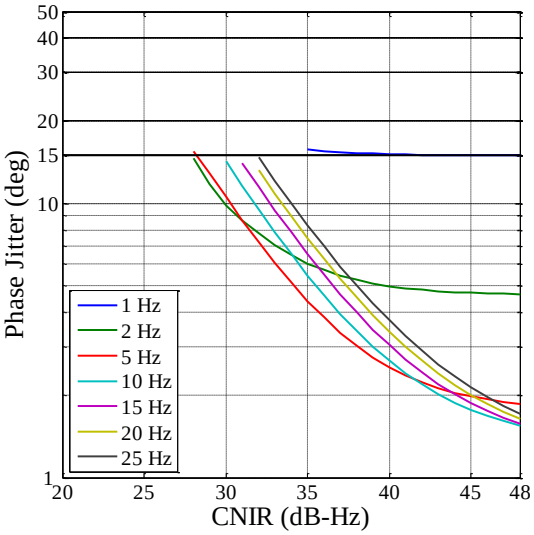

Figure 11: Phase jitter against CNIR for different loop bandwidths (with loop aiding). Results obtained using simulated data.

5.2 Aided loop performance

For determining the performance of loop aiding, noise+interference was introduced randomly at one of the two carrier frequencies. The signals at the other frequency were exposed to lower levels of noise+interference that allowed them to maintain higher CNIR levels (around 48 dB-Hz). As discussed above the loop with the best CNIR was selected in real-time as the aiding loop that operated with a wide B_L of 25Hz. The bandwidths of the aided loops ($B_{L(aided)}$) were varied in the range 1 – 25Hz over a number of simulations. Also, the CNIR of the signals at the affected frequency was varied in the range 25 – 48dB-Hz. This was done in order to explore the effects of aiding in various expected situations. Fig. 10 and 11 depict the situation after implementation of the proposed method. These figures are directly comparable to Fig. 8 and 9 (the same scales are used, explaining the relative sparseness of Fig. 8).

It can be observed from these figures that the aided loops at the affected frequency were able to maintain lock at B_L as low as 1Hz. This was possible due to the fact that the aided loops received signal dynamics estimates from the aiding loop. This allowed the aided loop to track only the residual errors as discussed in section 4 above and it didn't have to track the full platform dynamics which would have required a wider B_L. Below this B_L, the loop

was not able to maintain lock at any of the tested CNIR values.

This threshold of 1Hz for loss of lock was the same for CNIR≥35dB-Hz because the curves for these CNIR values converged at this point. The shifting of the threshold crossing and convergence point to a lower B_L value can be explained as follows: In the unaided case, errors due to signal dynamics dominated at 9Hz as compared to noise- and interference-induced errors. However, in the case of aided loops, errors due to signal dynamics were reduced by removing the burden of tracking full signal dynamics from the aided loop. Signal dynamics thus did not become dominant again until the noise- and interference-induced errors became much weaker at 1Hz. For signals with CNIR<35dB-Hz, tracking loops lost lock at $B_{L(aided)}$<2Hz due to increased levels of received noise and interference as compared to signals with CNIR≥35dB-Hz.

Also note that the fact that the effects of signal dynamics are reduced is also confirmed by the movement of the minimum jitter point from a higher B_L to a lower B_L for signals with reduced CNIR.

A comparison of Fig. 8 and 10 shows that using loop aiding, jitter reduction was also achieved for the aided signals with a high CNIR values. This was mainly due to the fact that for signals with higher CNIR, total phase jitter is mainly contributed by the signal dynamics. With loop aiding, effects of signal dynamics errors were mitigated that resulted in the total phase jitter reduction.

Looking at the situation in a different way, Fig. 11 shows the phase jitter values plotted against CNIR for the aided loop operating at different B_L. It was observed that for wider $B_{L(aided)}$, the aided loop was able to maintain lower jitter at higher CNIR. This can be observed by considering the curve of $B_{L(aided)}$=2Hz and 5Hz as compared to the curves for $B_{L(aided)}$>5Hz. However, at lower values of CNIR, the loop with the wider B_L lost lock before the one with a narrower B_L. This was due to the fact that at wider B_L jitter due to noise and interference dominates, which keeps the loop from maintaining lock at low CNIR values.

The margin achieved against received noise and interference can be noted by considering the plotted results. Fig. 9 shows that in an unaided situation, with a B_L of 15Hz, the 15° theoretical limit is exceeded when the signal level dropped below 33dB-Hz. However, it can be seen from Fig. 11 that this jitter value was not exceeded until the signal level dropped below 28 dB-Hz, while operating with a B_L of 2Hz. This shows that a margin of 5dB-Hz was achieved, under simulation conditions, against received wide band noise+ interference.

5.3 $B_{L(aided)}$ selection

The previous discussion suggested that loop aiding is employed to facilitate reduction in $B_{L(aided)}$ for the discussed reasons. Results presented above show that although tracking was possible down to a $B_{L(aided)}$ of 1Hz, the aided loop produced jitter near 15° with this bandwidth. This situation was highly vulnerable to any increase in signal dynamics or level of received noise and interference. Also, the maximum margin against CNIR was also not achieved at this minimum bandwidth but by operating with a $B_{L(aided)}$ of 2Hz. Also, for higher CNIR values, it can be noted that jitter at this minimum

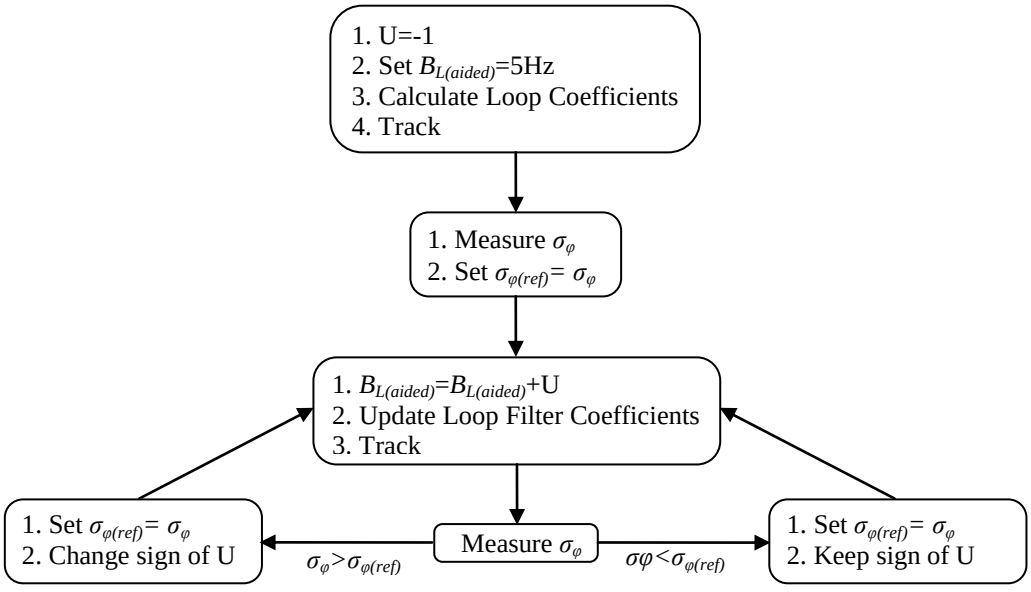

Figure 12: $B_{L(aided)}$ selection algorithm

bandwidth was higher than that at larger values of $B_{L(aided)}$. This suggests that the aided loop should not be operated with the minimum possible bandwidth but an adaptive selection of $B_{L(aided)}$ is necessary for maximizing this margin and minimising the jitter. Fig. 12 suggests a simple algorithm for this selection. According to this algorithm,

7. Initially the $B_{L(aided)}$ is set as 5Hz, and an update variable U is selected as -1. The loop filter coefficients are calculated using $B_{L(aided)}$ and tracking is performed.
8. The resulting jitter σ_{φ} is stored as $\sigma_{\varphi(ref)}$.
9. The $B_{L(aided)}$ is then updated by adding U to it, loop filter coefficients are recalculated and the tracking is continued.
10. The resulting jitter σ_{φ} is then calculated and compared against previous jitter (saved as $\sigma_{\varphi(ref)}$).
11. Sign of U is changed if the current jitter value (σ_{φ}) is more than the previous jitter value ($\sigma_{\varphi(ref)}$), otherwise it is kept same.
12. The process from step 2 repeats.

This algorithm continuously updates $B_{L(aided)}$ and compares the current jitter with the previous jitter value. If the jitter is found to be decreased, and this decrease was due to reduction in $B_{L(aided)}$, this bandwidth is reduced further. On the other hand, if the jitter is found to be increase, the direction of $B_{L(aided)}$ update is reversed to achieve a lesser jitter. This continuous updating of the $B_{L(aided)}$ value keeps the jitter at minimum. This algorithm is employed for achieving the rest of the results presented in this paper.

5.4 Impact of the aiding carrier's quality on aided loop's performance

To this point the aiding loop has been assumed to track a high CNIR signal. This was made possible by introducing lower levels of noise+interference into carriers at one of the two frequencies for keeping their CNIR high. In a real-world scenario it may not be the case that higher CNIR levels are always experienced for atleast one of the four carriers. It is highly likely that CNIR would degrade and/or fluctuate due to various factors including received noise and interference and multipath. It may be the case that the interference is received at both of the frequencies or the multipath affects signals at both frequencies and/or from both antennas. In this case CNIR will be reduced for the signals tracked by all the loops. As discussed above, the proposed scheme selects the loop tracking the carrier with the least amount of noise as the aiding loop. Due to the corruption of both the frequencies the loop selected for aiding will still be tracking a degraded signal.

To evaluate the performance of the proposed architecture in such a situation, the aiding loop was made to track signals with degraded CNIR values. Interference was assumed to be present at both the frequencies. This made

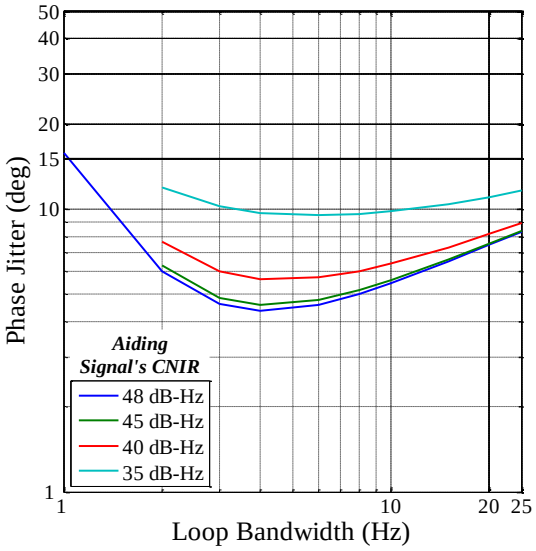

Figure 13: Phase jitter against $B_{L(aided)}$ for different $CNIR_{(aiding)}$ (with loop aiding). Interference affecting both aided and aiding loops. Results obtained using simulated data.

the aiding signal's CNIR degrade from a high value. For this test, the aided and the aiding loop were operated with 2Hz and 25Hz B_L respectively. CNIR of the signal tracked by aiding loop was varied in the range 35 – 48dB-Hz, while for the aided loop it was kept fixed at 35dB-Hz.

Performance of the aided loops, in this situation, in terms of phase jitter is depicted in Fig. 13. An interesting point to note here is that, in this case, the minimum achievable jitter (MAJ) value increased as the aiding loop signal's CNIR decreased. The observed increase in the MAJ is in accordance with Equation (9). As expected, a relationship between the quality of the signal tracked by the aiding loop and the performance achievable by the aided loop can be easily noted here.

Another interesting point to note here is that the aided loop's performance at wider $B_{L(aided)}$ was degraded mainly due to the fact that the wider $B_{L(aided)}$ allowed more noise to leak in from the degraded quality aiding signal. On the other hand, when the aided loop was operated with a narrower $B_{L(aided)}$ to reject the incoming noise, it was not able to track the residual signal dynamics error well which again resulted in an increase of phase jitter.

The observations discussed above, and the fact the aided loop's performance is dictated by the aiding signal quality, suggest that a lower limit on the aiding loops' performance needs to be set in order to gain advantage from the proposed method.

6. Adaptive Kalman Filter based Loop Aiding

Results presented above show that an aided loop can potentially reduce an aided loop's phase jitter by a margin in signal level of 5dB-Hz. However, some residual noise still leaks through the aided loop's narrow filter. This residual noise is contributed not only by the received noise entering the aided loop but also by that from the aiding loop, as discussed in the previous sections and depicted by the simulation results. This suggests that there exists room for improvement in terms of noise rejection in the aided loop's measurements. This improvement can be achieved if the noise present in the aiding loop's estimates can be mitigated before reaching the aided loops. The authors propose to employ a Kalman filter based implementation of the above proposed inter-loop aiding scheme to achieve this goal. For a standalone PLL, a Kalman filter (KF) has also been extensively researched to provide carrier phase measurements with reduced noise (Psiaki et al., 2001), (Psiaki et al., 2002), (Kim et al., 2008). Typically a KF either reduces noise in a loop filter's estimates or replaces the loop filter altogether to generate less noisy estimates. In order to improve further the performance of the above proposed scheme, an adaptive Kalman filter based architecture is employed where a cascade of KF replaces the individual loop filters of the four loops tracking carriers from the same LocataLite.

6.1 Kalman filter basics

Kalman filtering is a common approach for estimating the state of a noisy process. The KF achieves this objective by employing an iterative-in-time prediction-correction model represented by the following model equations:

1. Prediction Model:

$$\begin{aligned} \hat{x}_k^- &= A\hat{x}_{k-1} + Bu_k \\ P_k^- &= AP_{k-1}A^T + Q \end{aligned} \tag{10}$$

2. Correction Model:

$$\begin{aligned} K_k &= P_k^- H^T \left(HP_k^- H^T + R\right)^{-1} \\ \hat{x}_k &= \hat{x}_k^- + K_k\left(z_k - H\hat{x}_k^-\right) \\ P_k &= \left(I - K_k H\right)P_k^- \end{aligned} \tag{11}$$

Here x denotes the state vector to be estimated, hat symbol denotes the estimated element, superscript-minus ($^-$) indicates *a priori* nature of the element, A is the state transition matrix, B is the input matrix, P is the error covariance, K is the Kalman gain, z is the measurement vector, H is the measurement matrix and Q and R denote the covariances of the process noise w and measurement noise v respectively. Here the modelled noise statistics Q and R tune the Kalman filter for smooth tracking. The accuracy of these noise models, which potentially contribute to the performance of the KF, depends on *a priori* knowledge of system application and process dynamics, which is difficult to obtain in practice (Mohamed et al., 1999). Therefore approximate models can serve as a possible solution in such situations. However, during sudden manoeuvres, like rapid changes in trajectory (for instance, sharp turns), such models cannot replicate dynamics accurately leading to divergence of the KF, causing "overshoots". This happens due to the fact that the KF tries to maintain the previous trajectory and takes time to adjust to sudden changes. Adjusting these approximations can either "tighten" the Kalman filter, resulting in higher noise rejection and generating overshoots, or vice versa. This is a classic trade-off between dealing with dynamics and rejecting noise, and is discussed in detail in (Khan et al., 2009). In such cases an adaptive KF algorithm provides a better solution at the expense of increased complexity. An adaptive Kalman filter (AKF) dynamically adjusts the modelled noise statistics by estimating Q and/or R "on the fly". One possible approach to determine Q and R can be given as follows: Defining the measurement innovation v_k, as the difference between the actual measurement and its predicted value, it can be given as:

$$v_k = z_k - H\hat{x}_k^- \tag{12}$$

Using Equation (12), the innovation covariance matrix is:

$$C_k = E\left(v_k v_k^T\right) = HP_k^- H^T + R_k \tag{13}$$

This innovation covariance matrix can be employed to obtain Q and/or R using the following relationships (Mohamed et al., 1999):

$$\begin{aligned} R_k &= C_k - HP_k^- H^T \\ Q_k &= K_k C_k K_k^T \end{aligned} \tag{14}$$

Another trade-off involved here is the Kalman filter update rate. A faster update (e.g. with each loop update) may not allow loop parameters to settle to steady state. Alternatively, a slower update (e.g. 1Hz) may use *old* data and diminish the effects of any changes in measurements at the Kalman filter output). For this reason, the work reported in this paper considers a medium loop update rate of 20Hz.

6.2 Proposed scheme augmentation

To reduce the aided loop's residual noise in two stages, a cascade of Adaptive Kalman filters is employed for performing loop aiding. This cascade combines carrier phase error measurements from all four carrier loops tracking signals from the same LocataLite and generates the less noisy state estimates: carrier tracking error ($\delta\varphi$)

and carrier NCO updates (φ') for the aiding and the aided loops by minimising the error covariance of these estimates. First, based on the correlator outputs, CNIR is computed for each loop and the loop with the best CNIR is selected as the aiding loop. The correlator outputs of the loop selected for aiding are then used to generate carrier phase error measurements. As discussed above, where the noise and RFI are received on both of the frequencies, this corruption also degrades the phase error measurements generated by the aiding loop. The first filter of the cascade operates on these noisy carrier error measurements and estimates less noisy carrier NCO updates for this loop. These updates are then also used to produce the signal dynamics estimates for the aided loops using the ratio of the aiding and the aided signal's carrier frequencies. At this stage, the first KF not only reduces noise in the aiding loop's NCO updates, but also mitigates the noise in the aiding estimates. This helps reduce the noise entering the aided loops via the aiding loop. The aided loops' carrier tracking error measurements and the signal dynamics estimates originating from the aiding loop serve as input for the second filter that estimates carrier NCO updates for the aided loops. As both of these two inputs are corrupted by the residual noise as discussed in the previous section, the second KF operates to reduce this residual noise and generates smoothed updates for the aided loops. A KF based tracking architecture is shown in Fig. 14. The state vectors x , state transition matrixes A and input matrixes B for the first and second KFs of the cascade are proposed as follows:

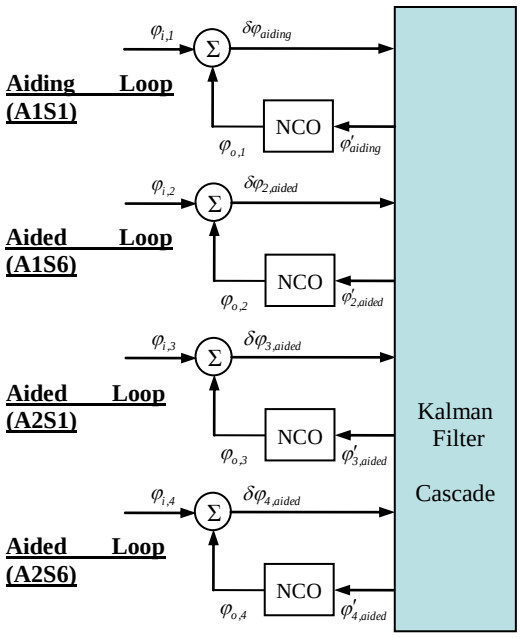

Figure 14: Kalman filter based loop aiding implementation.j

Kalman Filter 1:

$$x_1 = \begin{bmatrix} \delta\varphi_{aiding} \\ \varphi'_{ai\,dim\,g} \end{bmatrix}$$

$$A_1 = \begin{bmatrix} 1 & 0 \\ -\dfrac{\tau_2}{\tau_1}\Big)_{aiding} & 1 \end{bmatrix} \qquad (15)$$

$$B_1 = \begin{bmatrix} 0 \\ \dfrac{\tau_2 + T}{\tau_1}\Big)_{aiding} \end{bmatrix}$$

Kalman Filter 2:

$$x_2 = \begin{bmatrix} \delta\varphi_{2,aided} \\ \varphi'_{2,aided} \\ \delta\varphi_{3,aided} \\ \varphi'_{3,aided} \\ \delta\varphi_{4,aided} \\ \varphi'_{4,aided} \end{bmatrix}$$

$$A_2 = \begin{bmatrix} 1 & 0 & 0 & 0 & 0 & 0 \\ -\dfrac{\tau_2}{\tau_1}\Big)_{2,aided} & 1 & 0 & 0 & 0 & 0 \\ 0 & 0 & 1 & 0 & 0 & 0 \\ 0 & 0 & -\dfrac{\tau_2}{\tau_1}\Big)_{3,aided} & 1 & 0 & 0 \\ 0 & 0 & 0 & 0 & 1 & 0 \\ 0 & 0 & 0 & 0 & -\dfrac{\tau_2}{\tau_1}\Big)_{4,aided} & 1 \end{bmatrix}$$

$$B_2 = \begin{bmatrix} 0 & 0 & 0 & 0 & 0 & 0 \\ \dfrac{\tau_2 + T}{\tau_1}\Big)_{2,aided} & \beta_2 & 0 & 0 & 0 & 0 \\ 0 & 0 & 0 & 0 & 0 & 0 \\ 0 & 0 & \dfrac{\tau_2 + T}{\tau_1}\Big)_{3,aided} & \beta_3 & 0 & 0 \\ 0 & 0 & 0 & 0 & 0 & 0 \\ 0 & 0 & 0 & 0 & \dfrac{\tau_2 + T}{\tau_1}\Big)_{4,aided} & \beta_4 \end{bmatrix} \qquad (16)$$

here τ_1 and τ_2 denote the carrier loop coefficients, T denotes the pre-detection integration duration and β denotes the carrier frequency dependent scaling factor. The process noise models for the first and second KFs can be given as:

$$w_1 = \begin{bmatrix} \sigma^2_{\delta\varphi_1} & \sigma^2_{\varphi'_1} \end{bmatrix}^T$$

$$w_2 = \begin{bmatrix} \sigma^2_{\delta\varphi_2} & \sigma^2_{\varphi'_{2,m}} & \sigma^2_{\delta\varphi_3} & \sigma^2_{\varphi'_{3,m}} & \sigma^2_{\delta\varphi_4} & \sigma^2_{\varphi'_{4,m}} \end{bmatrix}^T \qquad (17)$$

where $\sigma^2_{\delta\varphi_n}$ and $\sigma^2_{\varphi'_n}$ define carrier tracking error and carrier NCO update estimation process noise respectively, and m denote the aiding loop.

By definition, the process and the measurement noise statistics are:

$$\begin{aligned} P(w) &\sim N(0,Q) \\ Q &= E\left[w_k {w_l}^T\right] \\ P(v) &\sim N(0,R) \\ R &= E\left[v_k {v_l}^T\right] \end{aligned} \tag{18}$$

6.3 Performance evaluation and comparison

This sub-section analyses the PLL performance for the above mentioned scenarios, discussed in Section 5.2, using an AKF-based loop aiding (LA-AKF) architecture. This architecture offers various different advantages as discussed below:

Improvement in terms of MAJ. First consider the scenario where the aiding loop operates with a bandwidth of 25Hz while tracking a signal with a high CNIR. A high value of CNIR was chosen again to consider the situation where the interference is received potentially on only one of the frequencies and/or the multipath was not affecting the antenna transmitting the carrier tracked by the aiding loop. The performance of the aided loop is evaluated for bandwidths up to 25Hz while tracking signals with different CNIR. Fig. 15 and 16 show the results where the loop performance is plotted in terms of phase jitter against $B_{L(aided)}$ and tracked signal's CNIR. It was observed that the LA-AKF was unable to operate at B_L less than 1Hz, as was the case with the aided loop without Kalman filter (LA-NKF). However the main point of concern will be the improvement in terms of minimum achievable jitter (MAJ) while tracking the signals with low CNIR. By comparing Fig. 15 with Fig. 10 it can be noted that the LA-AKF further reduced the MAJ compared to the LA-NKF. For example, for the 35dB-Hz signal, the LA-AKF was able to track with an MAJ value of 2.8° as compared to the LA-NKF which tracked the same signal with an MAJ value of 4.3°. Also, the LA-AKF was able to maintain a lower phase jitter value at higher $B_{L(aided)}$ for all tested CNIR values. This reflects the effects of AKF based implementation on the performance of the aided loop. The signal tracked by the aiding loop was of high quality, so use of AKF did not have much effect in terms of noise rejection in aiding estimates. Therefore any reduction in MAJ as compared to LA-NKF was contributed by the rejection of noise present in the aided signal itself.

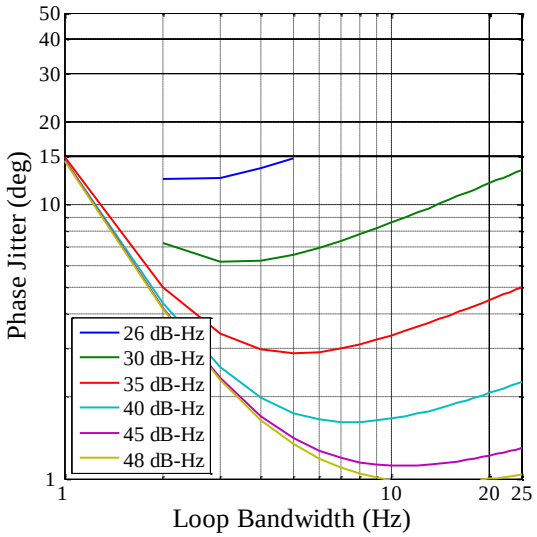

Figure 15: Phase jitter against loop bandwidth for different CNIR (with LA-AKF). Results obtained using simulated data.

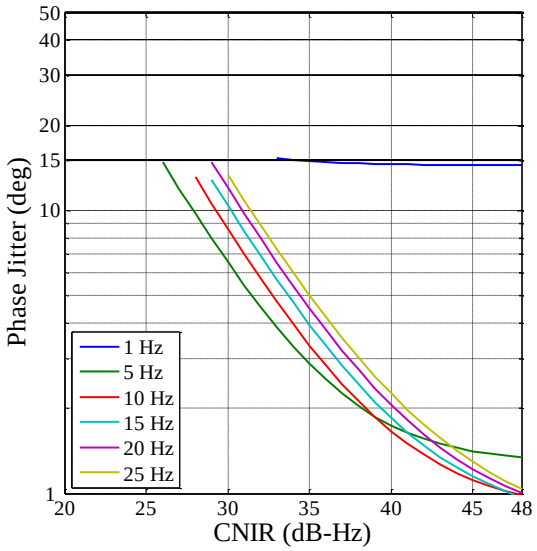

Figure 16: Phase jitter against CNIR for different loop bandwidth (with LA-AKF). Results obtained using simulated data.

Further Improved Margin against RFI. Analysing the improvement from another perspective, a comparison of Fig. 16 and 11 illustrates that while the LA-NKF tracked signals with a minimum CNIR value of 28dB-Hz, the LA-AKF was able to track signals down to a CNIR of 26dB-Hz before it crossed the 15° phase jitter threshold, offering a margin of further 2dB-Hz over the LA-NKF under same simulation conditions. Also at moderate CNIR values, the LA-AKF performed better than the LA-NKF, as can be noted by comparing Fig. 16 and 11. These improvements were achieved mainly due to the fact that in the case of the LA-AKF, not only the aided loops rejected noise by operating at a smaller B_L, but also the aiding loop estimates were made less noisy using the

AKF, before these were injected into the aided loop. The second stage KF in the KF cascade also contributed to this improvement by statistically minimising the error covariance during the aiding process. There is a significant point to note here. In the case of the LA-NKF, jitter due to received noise and interference can be reduced by decreasing the aided loop's bandwidth. However, this is at the cost of making the loop more vulnerable to signal dynamics. The LA-AKF offers improvement in rejecting incoming noise and interference without making the loop vulnerable to signal dynamics and loss of lock as the LA-AKF does not require further reductions in loop bandwidths.

Resistance against an aided loops' performance degradation while the aiding signal quality degrades. This subsection considers a harsher scenario, where the aiding signals' CNIR degraded from a higher value and was tracked with $B_{L(aiding)}$=25Hz. For the set of results presented in this section the aided signal was kept at 35dB-Hz CNIR. Fig. 17 illustrates these results. Some important observations can be made here by comparing this figure with the LA-NKF results presented earlier in Fig. 13. It can be noted that even though the aiding signal quality degraded, the LA-AKF architecture allowed lesser jitter increment, for the aided loop, than the LA-NKF architecture. This was mainly due to the fact that this time the AKF cascade not only mitigated the noise in the aided signal itself but also that present in the aiding estimates.

Due to the fact that a corrupted aiding signal can degrade an aided loop's performance, it was identified in Section 5c that a lower limit needed to be set on the aiding signal quality so that the aided loop's performance remains within acceptable limits. The fact that the LA-AKF

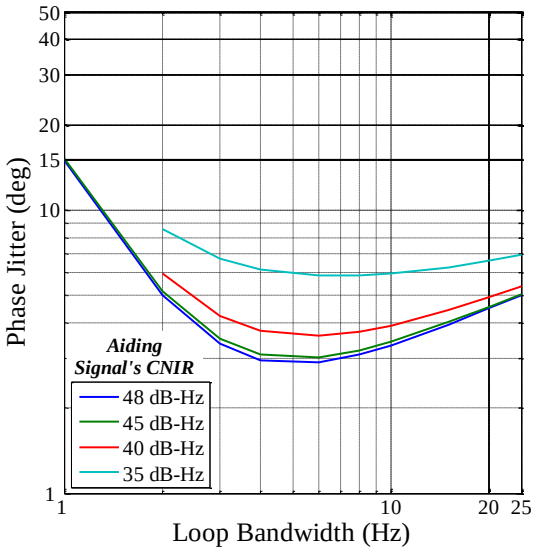

Figure 17: Phase jitter against $BL_{(aided)}$ for different $CNIR_{(aiding)}$ (with LA-AKF). Interference affecting both aided and aiding loops. Results obtained using simulated data.

performance, as compared to that of the LA-NKF, degrades less while the aiding signal quality is corrupted by same amount of noise and interference, suggests that this limit can be further lowered and an even lower quality signal can be used for aiding.

7. Real Data Results:

In order to validate the proposed scheme, real Locata IF samples were collected using a National Instruments PXI 5142 digitiser. In order to collect clean signals, the LocataLite was set to transmit at the highest possible power level. The wide band noise was later added artificially (numerically in Matlab). This was done in order to achieve desired CNIR levels, and to conduct the experiments in a controlled environment. Both transmitter (TX) antennas (A1 and A2) were mounted on a fixed tripod stand and the receiver (RX) antenna was mounted on a portable stand. This portable stand allowed movement of the RX antenna in order to introduce the dynamics. Each of the Locata signals is 20 MHz wide and simultaneous sampling of signals at both the frequencies requires at least a sampling frequency of 80MHz, resulting in a large number of collected samples for a given duration of observation. This posed serious limitations on the amount of data that could be collected; memory limitations allowed data collection only for short durations. In such short durations, it was possible to introduce dynamics less than 0.38g/s – a value used for simulation results. It is to be noted that multipath will be present in the received signals due to the indoor location of the experiment setup.

First the unaided loop's results are presented to evaluate the loop performance in the absence of aiding. The results are depicted in Figures 18 and 19. It can be observed that the loop was unable to track signals with CNIR <34dB-Hz. Also, as the B_L was reduced to reject the noise, tracking was not possible below B_L=11Hz.

The loop aiding architecture was then employed and it can be noted from Fig. 20 and 21 that the minimum usable B_L value improved to 3Hz allowing further noise rejection. Fig. 21 shows that tracking was possible down to 30dB-Hz. This validates the proposed loop aiding scheme that in this case offers a margin of 4dB-Hz against noise. Improvement in MAJ can also be observed by comparing Fig. 18 and 20. Again, in this case, lower levels of noise were introduced at one of the frequencies, keeping the aiding signal's CNIR levels high at that frequency. When potential interference was introduced at both of the frequencies, the aiding loop was also affected. The effects of noise were reflected in the aided loops' performance. This situation is depicted in Fig. 22, where the aided loop tracked the signal with CNIR=35dB-Hz, while the CNIR levels of the aiding signal varied between the 35 – 48dB-Hz range. This is in

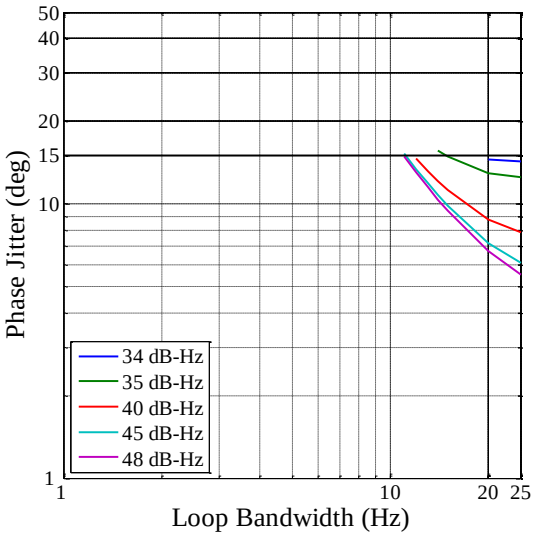

Figure 18: Phase jitter against loop bandwidth for different CNIR (without Loop Aiding). Results obtained using real data and simulated noise.

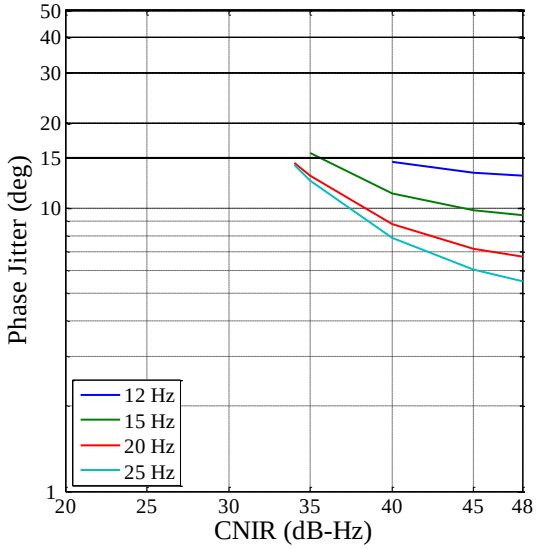

Figure 19: Phase jitter against CNIR for different loop bandwidths (without loop aiding). Results obtained using real data and simulated noise.

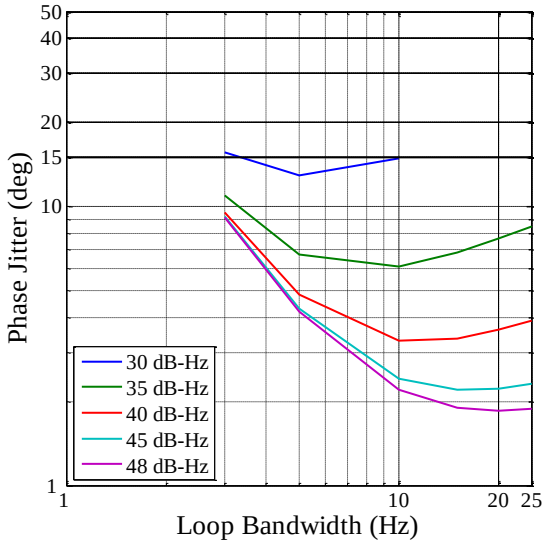

Figure 20: Phase jitter against loop bandwidth for different CNIR (with LA-NKF). Results obtained using real data and simulated noise.

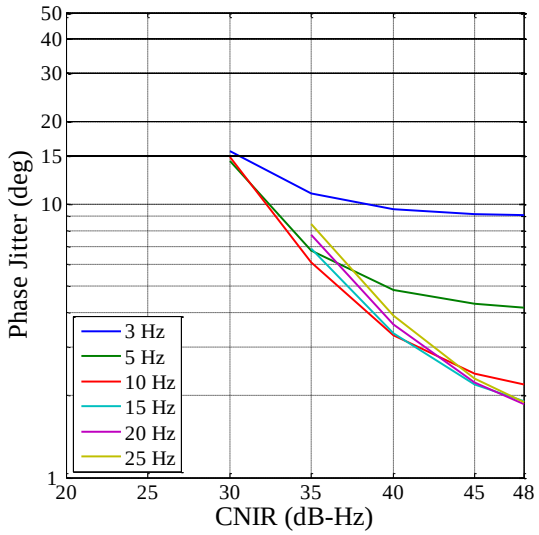

Figure 21: Phase jitter against CNIR for different loop bandwidths (with LA-NKF). Results obtained using real data and simulated noise.

agreement with the observations made using the simulation results (depicted in figure 13).

In order to mitigate the effects of degrading aiding signal quality on an aided loop's performance, the AKF based loop aiding architecture was employed. At first the case of a high quality aiding signal is considered and the phase jitter obtained is plotted in Fig. 23 and 24 against $B_{L(aided)}$ and CNIR. Similar observations can be made here as in the case of the simulation results. First, the minimum trackable CNIR improves from 30dB-Hz (in case of LA-NKF for real data) to 27dB-Hz in this case. In addition, the MAJ improves by using LA-AKF as compared to LA-NKF. Considering the case of a lower quality aiding signal, the situation is depicted in Fig. 25. A comparison of Fig. 24 with Fig. 22 shows that, as compared to an LA-NKF architecture, the LA-AKF architecture improves an aided loop's performance as the aiding signal quality degrades.

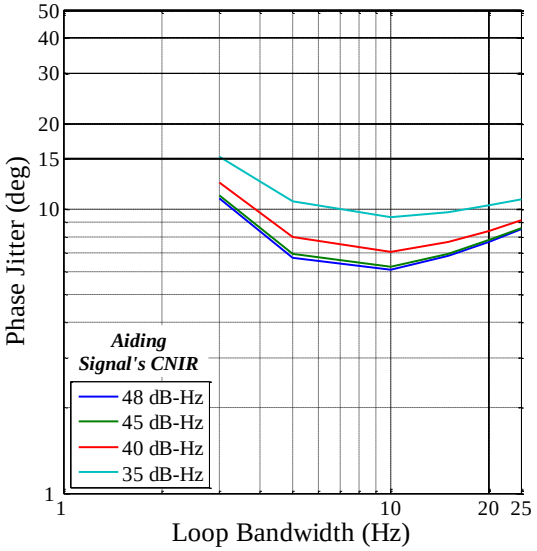

Figure 22: phase jitter against $B_{L(aided)}$ for different $B_{L(aiding)}$ (LA-NKF). Interference affecting both aided and aiding loops. Results obtained using real data and simulated noise.

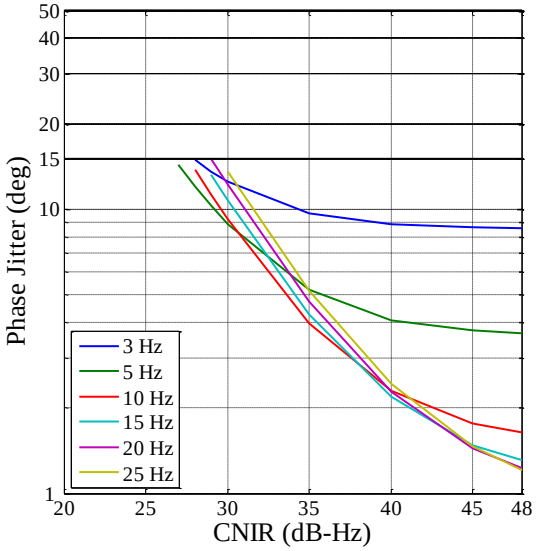

Figure 24: Phase jitter against CNIR for different loop bandwidths (LA-AKF). Results obtained using real data and simulated noise.

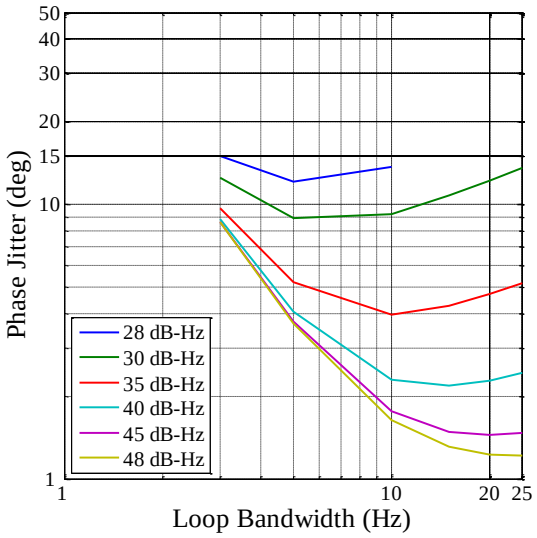

Figure 23: Phase jitter against loop bandwidth for different CNIR (LA-AKF). Results obtained using real data and simulated noise.

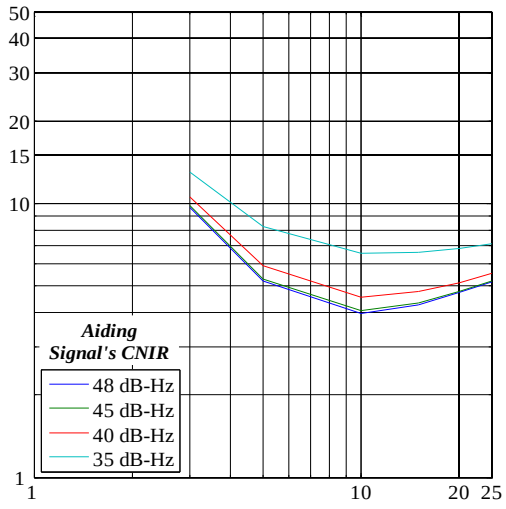

Figure 25: Phase jitter against $B_{L(aided)}$ for different $B_{L(aiding)}$ (With LA-AKF). Interference affecting both aided and aiding loops. Results obtained using real data and simulated noise.

8. Conclusion:

An adaptive inter-loop aiding scheme is proposed and analysed using detailed simulations and real data. The proposed scheme's performance is evaluated with and without the use of an Adaptive Kalman filter based implementation. This scheme employs the concept of loop aiding without requiring any external estimates. It is established that the inter-loop aiding improves the tracking loop performance by reducing its phase jitter and allowing tracking of signals with CNIR values reduced by wide band noise and interference. It is identified that although loop aiding allows $B_{L(aided)}$ reduction, the aided loop does not necessarily need to operate with a minimum possible bandwidth. An algorithm is proposed that continuously selects $B_{L(aided)}$ that minimises jitter. Performance improvement is shown to be achieved when either or both of the carrier frequencies are affected by received noise and interference. It is shown using simulation and real data results that a margin of 4 – 5dB-Hz can be achieved

without using Adaptive Kalman filtering. It is identified that an adaptive Kalman filter-based implementation of the proposed scheme improves this margin by another 2 – 3dB-Hz. It is also established that, in the absence of the Kalman filter, the quality of the aiding signal will potentially dictate the quality of aiding, and eventually the aided loop's performance. Considering this fact it is shown that a lower bound is predictable for the aided loop's performance. It is also shown that Adaptive Kalman filter-based loop aiding improves the situation by mitigating the noise in the aiding estimates as the quality of the aiding signal degrades. It is also identified that in the case of the Adaptive Kalman filter-based aiding scheme improvements are obtained without making loops vulnerable to loss of lock, as the Adaptive Kalman filtering does not require further reduction in loop bandwidths.

Acknowledgement

This research is supported by Australian Research Council Linkage Projects LP0668907 and LP0560910.

References

Alban, S., D. M. Akos, S. M. Rock and D. Gebre-Egziabher (2003), ***Performance analysis and architectures for ins-aided GPS tracking loops***, National Technical Meeting of the U.S. Institute of Navigation, Anaheim, California, 22-24 January, pp. 611 – 622.

Barnes, J., C. Rizos, M. Kanli, A. Pahwa, D. Small, G. Voigt, N. Gambale and J. Lamance (2005), ***High accuracy positioning using Locata's next generation technology***, 18th Int. Tech. Meeting of the Satellite Division of the U.S. Institute of Navigation, Long Beach, California, 13-16 September, pp. 2049-2056.

Chiou, T., D. Gebre-Egziabher, T. Walter and P. Enge (2007), ***Model analysis on the performance for an inertial aided FLL-assisted-PLL carrier-tracking loop in the presence of ionospheric Scintillation***, National Technical Meeting of the Institute of Navigation, San Diego, California, 22 – 24 Jan, pp. 1276 – 1295.

Gebre-Egziabher, D., A. Razavi, P. Enge, J. Gautier, S. Pullen, B. Pervan, and D. M. Akos (2005), ***Sensitivity and performance analysis of Doppler-aided GPS carrier-tracking loops***, Navigation, Vol. 52, No. 2, pp. 49 – 60.

Fontana, R. D., W. Cheung and T. A. Stansell (2001), ***The new L2 civil signal***, 14th Int. Tech. Meeting of the Satellite Division of the U.S. Inst. of Navigation, Salt Lake City, Utah, 11-14 September, pp. 617-631.

Irsigler M. and B. Eissfeller (2002), ***PLL tracking performance in the presence of oscillator phase noise***, GPS Solutions, Vol. 5, No. 4, pp. 45-57.

Julien, O., (2005), ***Carrier-phase tracking of future data/pilot signals***, 18th Int. Tech. Meeting of the Satellite Division of the U.S. Institute of Navigation, Long Beach, California, 13-16 September, pp. 113–124.

Khan, F. A., A. G. Dempster and C. Rizos (2010), ***Locata performance evaluation in the presence of wide- and narrow-band interference***. Journal of Navigation, Royal Institute of Navigation, Vol. 63, No. 3. pp. 527 – 543.

Khan, F. A., A. G. Dempster, and C. Rizos (2009), ***Kalman filter based adaptive loop aiding for performance improvement in low C/(No+I) environments***, IGNSS Symposium. 2009, Gold Coast, Australia, 1-3 December, CD-ROM proceedings.

Kim K. H., G. I. Jee and J. H. Song (2008), ***Carrier tracking loop using the adaptive two-stage Kalman filter for high dynamic situations***, International Journal of Control, Automation, and Systems, Vol. 6, No. 6, pp. 948-953.

Megahed, D., C. O'Driscoll and G. Lachapelle (2009), ***Combined L1/L5 Kalman filter-based tracking for weak signal environments***, ATTI dell'Istituto Italiano di Navigazione, No 189, July Issue, pp. 45-56.

Mohamed A. H. and K. P. Schwarz (1999), ***Adaptive Kalman Filtering for INS/GPS***, Journal of Geodesy 73, 193 – 203.

Psiaki, M. L. and H. Jung (2002), ***Extended Kalman filter methods for tracking weak GPS signals***, 15th Int. Tech. Meeting of the Satellite Division of the U.S. Inst. of Navigation, Portland, Oregan, 24-27 September, pp. 2539-2553.

Psiaki, M. L. (2001), ***Smoother-based GPS signal tracking in a software receiver***, 14th Int. Tech. Meeting of the Satellite Division of the U.S. Inst. of Navigation, Salt Lake City, Utah, 11-14 September, pp. 2900-2913.

Qaisar, S. U. (2009), ***Performance analysis of Doppler aided tracking loops in modernized GPS receivers***, 22nd Int. Tech. Meeting of the Satellite Division of the U.S. Inst. of Navigation, *Sav*annah, Georgia, pp. 22-25 September, 209-218.

Razavi, A., D. Gebre-Egziabher, D. M. Akos (2008), ***Carrier loop architectures for tracking weak GPS signals***, IEEE transactions on aerospace and electronic systems, Vol. 44, No. 2, pp. 697 – 710.

Singh, J., S. Singh and E. Joneson (1996), ***Measurement and analysis of US truck vibration for leaf spring and air ride suspensions, and development of tests to simulate these conditions***, Journal of Packaging Technology and Science, vol. 19, no. 6, pp. 309-323.

Ward, P., J. W. Betz, and C. J. Hegarty (2006), ***Satellite signal acquisition, tracking, and data demodulation* in GPS: Principles and Applications**, 2nd Edition, Artech House Publication.

Appendix I – Contributions of the aiding and aided loops for generating aided loop's estimates

In order to determine the proportion of contributions made by the aiding and aided loop to constitute the aided loop's estimated output phase φ_o, a conventional approach can be employed. First consider the situation for an unaided loop, as shown in Fig. 26. Here $\theta_i(z)$ denotes the phase of the input signal and $\theta_o(z)$ $(=Z\{\varphi_o\})$ denotes the phase of the VCO output. The phase detector generates a voltage signal ($V_d(z)$) proportional to the difference between the received and the estimated phases:

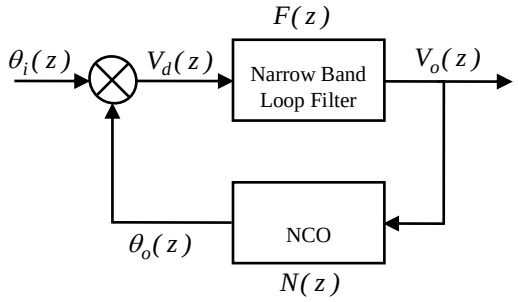

Figure 26: A conceptual unaided PLL.

$$V_d(z) = K_d(\theta_i(z) - \theta_o(z)) \tag{A.1}$$

where K_d is the gain of the phase detector. This voltage signal is filtered using the loop filter $F(z)$ for suppressing noise and higher frequency components and the resulting voltage signal $V_c(z)$ $(=F(z)V_d(z))$ is used to control the VCO. In the simulations that follow a software based receiver is used, where the VCO is replaced by an NCO for which the transfer function is:

$$N(z) = \frac{K_o z^{-1}}{1 - z^{-1}} \tag{A.2}$$

where K_o denotes the NCO gain. The NCO here amplifies the received signal using the gain factor K_o and integrates the resulting signal to generate the estimated output phase $\theta_o(z)$.

This conventional loop can be modified to obtain the desired expression for the aided loop's estimated output phase. The loop aiding architecture is illustrated in Fig. 27. From this figure, estimated output phase $\theta_o(z)$ for the aided loop can be given as:

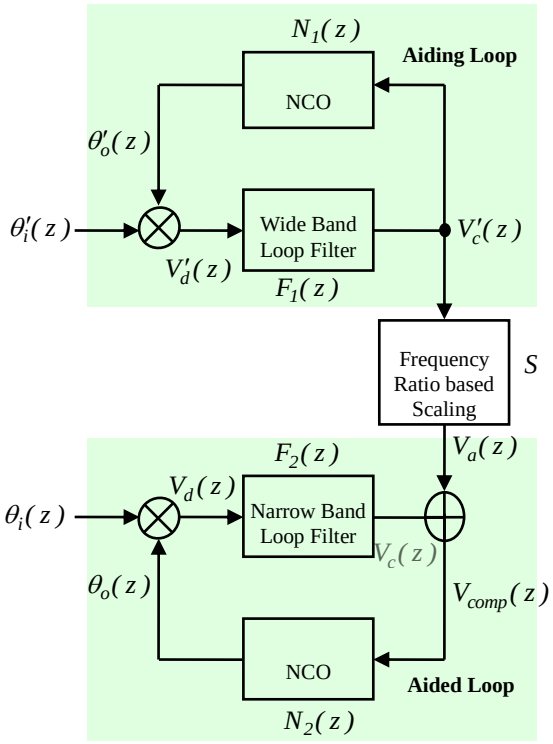

Figure 27: A conceptual inter-loop aiding architecture.

$$\theta_o(z) = N_2(z)V_{comp}(z) \tag{A.3}$$

here, $V_{comp}(z)$ is the composite voltage given by:

$$V_{comp}(z) = V_a(z) + V_c(z) \tag{A.4}$$

where
$$V_a(z) = SV_c'(z) \tag{A.5}$$

$$S = f_{aided} \Big/ f_{aiding} \tag{A.6}$$

$V_c'(z)$ is the voltage signal proportional to the aiding loop's signal dynamics and $V_c(z)$ is the voltage signal

proportional to the aided loop's estimate of residual signal dynamics that it tracks. Now, Equation (A.3) can be expanded using Equation (A.4) to give:

$$\theta_o(z) = N_2(z)(V_a(z) + F_2(z)V_d(z)) \quad \text{(A.7)}$$

Also, by using Equation (A.1), Equation (A.7) can be rewritten as:

$$\theta_o(z) = N_2(z)V_a(z) + N_2(z)F_2(z)K_d(\theta_i(z) - \theta_o(z))$$
$$\theta_o(z) = N_2(z)V_a(z) + K_d N(z)F_2(z)\theta_i(z) - K_d N_2(z)F_2(z)\theta_o(z)$$
$$\theta_o(z) = \frac{N_2(z)V_a(z) + K_d N(z)F_2(z)\theta_i(z)}{1 + K_d N_2(z)F_2(z)}$$
$$\theta_o(z) = \frac{N_2(z)}{1 + K_d N_2(z)F_2(z)}V_a(z) + \frac{N_2(z)F_2(z)}{1 + K_d N_2(z)F_2(z)}V_i(z) \quad \text{(A.8)}$$

where $V_i(z)$ ($= K_d\theta_i(z)$) is the voltage signal proportional to the phase of the signal received at the input of the aided loop. Equation (A.8) represents the proportion in which aiding and aided loops' contributions are combined to constitute the aided loop's estimated output phase.

Biography

Faisal Ahmed Khan is currently a doctoral candidate at the School of Surveying & Spatial Information Systems, University of New South Wales (UNSW). His main area of research is interference effects analysis and mitigation. He holds a M.Phil. degree from UNSW, Australia, and a B.E. (Electronics) degree from NED UET, Pakistan. He has also gained hands-on experience in the field of satellite communications at Institute of Space Technology and the Pakistan Space and Upper Atmosphere Research Commission.